2014 5th IEEE RAS & EMBS International Conference on
Biomedical Robotics and Biomechatronics (BioRob)
August 12-15, 2014. São Paulo, Brazil

# Design and Preliminary Test Results of a Novel Microsurgical Telemanipulator System

R. Cau, F.B.F. Schoenmakers, M. Steinbuch, *Member, IEEE*, T.J.M. van Mulken and R.R.W.J. van der Hulst.

***Abstract*— In this paper a novel telemanipulator system is proposed, able to assist during reconstructive surgery procedures involving microsurgical techniques. The proposed solution is based on maintaining work methods and infrastructure in the operating room (OR). An extensive analysis of these conventional methodologies, combined with a review of currently available alternative solutions, has led to the design of a new 7DOF master-slave system. The modular design concept is focused on precision, safety, ease-of-use, and cost-efficiency. A proof-of-concept has been tested, whereas preliminary results indicate a bidirectional precision at the slave end effector of 70 µm. Through optimization of the control software, a bidirectional precision down to 30−40 µm can be achieved.**

## I. INTRODUCTION

Reconstructive surgery is focused on restoration of form and function of various parts of the body. It includes restoration of birth defects, hand surgery, maxillofacial surgery, and reconstruction of defects after tumor removal or severe accidents. The most complex form of reconstructive surgery involves transplantation of autologous tissue. A free flap is created by harvesting skin, fat, muscle, or bone tissue including blood vessels and nerves from a donor site on the patients own body. The free flap is transplanted to the site of the defect, its vessels and nerves are locally reconnected (microvascular anastomosis), and the tissue is remodeled to the original size and shape of the defect. Dependent on the volume of transplanted tissue, the diameter of the reconnected vessels and nerves ranges between 1.5 and 2.5 mm.

Anastomosis needs to be completed within a certain time to prevent necrosis of the transplanted tissue, and is performed by placing eight sutures around the circumference. The relative distance between these sutures significantly determines the success rate of microvascular anastomosis. Failed anastomosis may lead to (partial) flap loss, which implies that the patient is left with an additional defect on his or her body. Microvascular anastomosis requires microsurgical needles and instruments, a surgical microscope, and special surgical techniques.

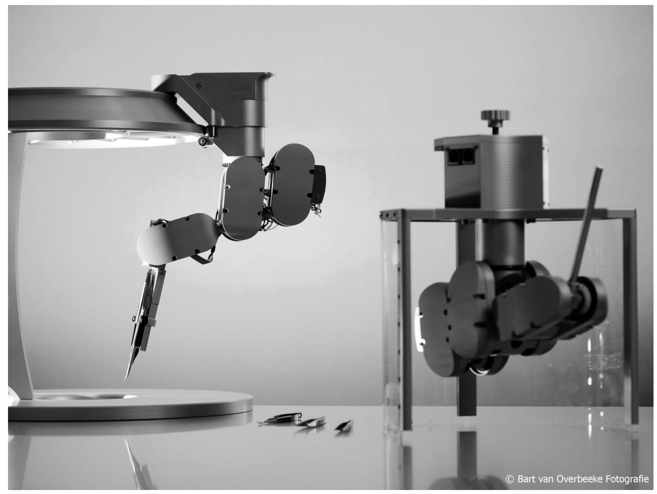


Fig. 1. The novel microsurgical telemanipulator system.

The surgical outcome that can be achieved using these techniques is dependent on the surgeon's motor skills and hand-eye coordination, yet limited by the effects of physiological tremor. Expert microsurgeons are able to limit the peak-to-peak amplitude of physiological tremor to 50 µm [1]–[3] in the fingertips, which is sufficient to successfully achieve anastomosis of vessels and nerves of 1.5 mm diameter. Lesser skilled surgeons need to resort to larger diameter vessels if present, or refrain from performing microsurgery. Anastomosis of vessel and nerve diameters smaller than 1.0 mm, as required for reconstructing fingertips or facial features, gives less reproducible surgical outcome and is thus only applied in experimental cases [4], [5].

Robotic assistance during microsurgical procedures could improve surgical precision, by offering motion scaling and tremor filtration. Several robotic systems have been developed for microsurgery [6]–[9].

Intuitive Surgical's DaVinci system has been tested in several procedures, with varying results [10]–[16]. The master-slave setup was found to be particularly useful in reducing tremor and facilitating the procedure in terms of ergonomics and accessibility. The absence of true microsurgical instruments, suitable for handling 9-0 or 10-0 needles, resulted in an increase in operating time. The telemanipulator did provide a more comfortable work

R. Cau, F. B. F. Schoenmakers, and M. Steinbuch are with the Eindhoven University of Technology (TU/e), P.O. Box 513, 5600 MB Eindhoven, the Netherlands (e-mail: r.cau@tue.nl; f.schoenmakers@tue.nl; m.steinbuch@tue.nl)
T. J. M. van Mulken and R. R. W. J. van der Hulst are with Maastricht University Medical Center (MUMC), P.O. Box 5800, 6202 AZ Maastricht, the Netherlands (e-mail: tomvanmulken@yahoo.com; r.vander.hulst@mumc.nl)
Contact author: M. Steinbuch (phone: 31-40-2475444; fax: 31-40-2461418; e-mail: m.steinbuch@tue.nl)

posture and a perceived higher precision through motion scaling. Using a DaVinci system to perform microsurgery requires drastic changes in workflow as well as in OR setup.

Mitsuishi et al. [17], [18] describe a microsurgical robotic system designed to perform anastomosis in neurosurgical fields. The system layout has been designed considering the OR infrastructure during superficial brain surgery procedures. End-to-end and end-to-side anastomoses of $0.3-0.5$ mm artificial blood vessels have been realized. This 6DOF master-slave system has been designed specifically for micro-neurosurgery, with dedicated microsurgical instruments and motion scaling allowing 30 µm accuracy in a workspace volume of $100\times100\times400$ mm. Compared to conventional microsurgery, task completion time was much longer.

This paper describes the design and development of a novel microsurgical telemanipulator system [19]. In collaboration with leading microsurgeons[1], and regarding results of existing microsurgical robotic platforms, a new set of requirements have been formulated. This has led to a new design concept and the realization of a proof-of-concept of a compact modular system, of which the first test results are presented.

## II. Methods

### A. Definition of requirements

An analysis of conventional microvascular anastomosis has been performed to determine the minimum performance requirements for the new system, as shown in Table I. The novel system combines proven methods of conventional microsurgery with the benefits offered by robotic technology. A large number of design specifications and attributes are left identical to those belonging to conventional microsurgery, thus creating an intuitive system that is easily integrated into the OR. The size and weight of the system are deliberately kept small, such that it does not require any significant changes in OR layout and planning.

### B. Mechanical Design

The design principles of the new system revolve around three key features, found in this order: safety, ease-of-use, and cost-efficiency. The system can be configured in a variety of setups. A setup consists of up to four master-slave combinations, in which the master manipulators are mounted to the surgical table and the slave manipulators are mounted to a suspension ring, as shown in Fig. 2. The suspension ring is mounted to a surgical microscope.

Compared to conventional microsurgery, the surgeons remain seated close to the patient. This allows them to use the existing surgical microscope, but also provides a safety barrier. The surgeon has a direct view of the patient and the operation site, at all times. In case of failure of any of the system's components, the surgeon is able to quickly switch to a manual approach. Master and slave manipulator mechanisms are identical. The manipulators are composed of three identical differential modules, serially linked between a manipulator base and an end effector (Fig. 3). The manipulator base is designed such that it can easily be attached or removed. The end effector link holds and actuates a genuine microsurgical instrument in 1DOF.

[1]From the Maastricht University Medical Center (MUMC) department of plastic, reconstructive, and hand surgery

TABLE I

SELECTION OF TECHNICAL SPECIFICATIONS OF THE NEW ROBOTIC SYSTEM, COMPARED TO CONVENTIONAL MICROSURGERY

| | **Conventional microsurgery** | **Microsurgical telemanipulator system** |
|---|---|---|
| Precision | 0.15 mm | 0.03 mm |
| Controllable DOF | 7* | 7 |
| No. of Manipulators | Up to 4 | Up to 4 |
| Type of Instruments | Microsurgical Instrument Set, sterilizable | Microsurgical Instrument Set, Sterilizable |
| Vision | Surgical microscope | Surgical microscope |
| Motion Scaling | - | $10-100\%$ |
| Tremor Filtering | - | $>4$ Hz |
| Size | - | $450\times450\times300$ mm |
| Mass | - | $<10$ kg |

* Measured from the surgeon's wrist

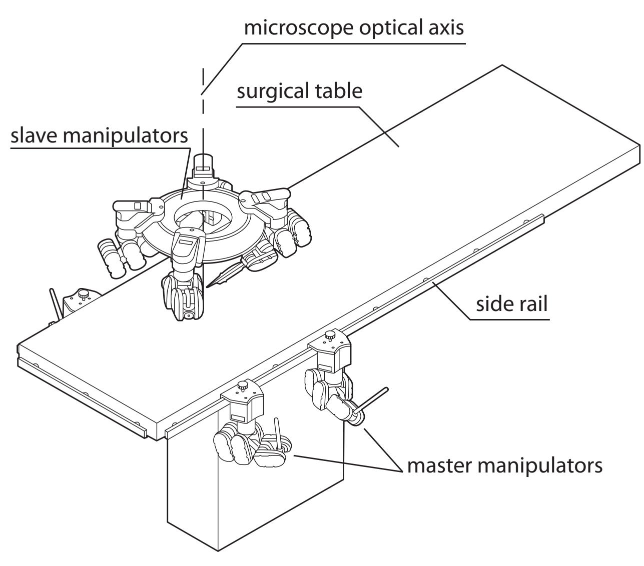


Fig. 2. Overview of the new telemanipulator system for microsurgery, in a configuration using four master-slave combinations.

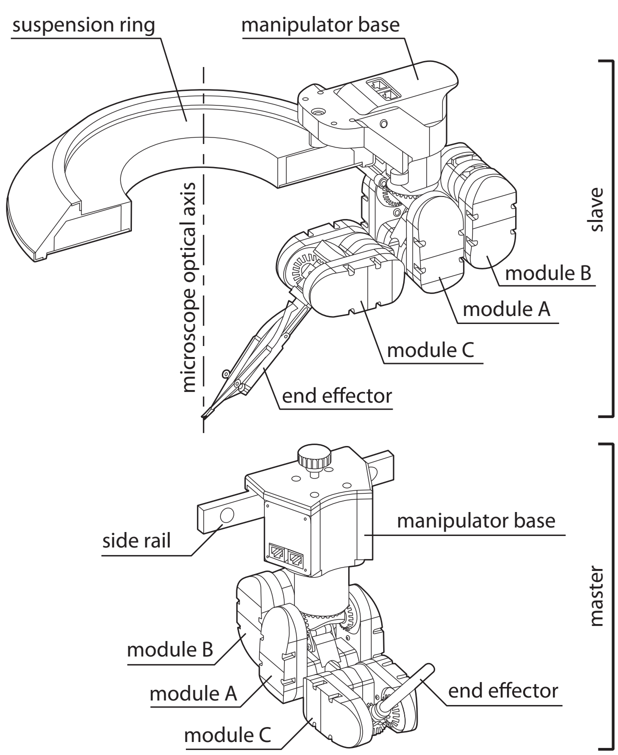


Fig. 3. Master and slave manipulators are both composed of three identical modules. The slave manipulator is able to hold and actuate a genuine microsurgical instrument and is mounted to a suspension ring which is connected to a microscope. The master manipulator is mounted to the side rail of a surgical table and has an instrument simulating end effector.

The newly developed differential modules each produce a fully backdrivable 2DOF output. The workspace and kinematic order of these modules is based on a human hand holding a microsurgical instrument, whereas the wrist of the hand is held steady. The layout of the manipulator links is such, that 6 out of 7 degrees of freedom are unaffected by gravity without using additional balancing masses. Each module contains a differential gear, which enables actuation of the outgoing gear in pitch ($\phi_{tool}$-axis) and roll ($\theta_{tool}$-axis) motion (Fig. 4).

### *C. Position Controller Design*

A module contains two dc motors, each of which drives one side of the differential gear via a transmission. Driving both motors in the same direction will rotate the outgoing gear of the differential gear around the roll-axis ($\theta_{tool}$-direction). Driving them in opposite direction causes the outgoing gear to rotate around the pitch-axis ($\phi_{tool}$-direction). Given a module with transfer function matrix $\boldsymbol{G_{mod}}$, with in- and outputs being the rotation of the two driven gears, $\boldsymbol{G_{mod}}$ can be decoupled by the input and output decoupling matrices $\boldsymbol{T_u}$ and $\boldsymbol{T_y}$:

$$\boldsymbol{L} = \boldsymbol{T_y G_{mod} T_u},$$

$$\boldsymbol{T_u} = \begin{bmatrix} 1 & 1 \\ 1 & -1 \end{bmatrix}, \quad \boldsymbol{T_y} = \begin{bmatrix} 0.5 & 0.5 \\ 0.5 & -0.5 \end{bmatrix} \qquad (1)$$

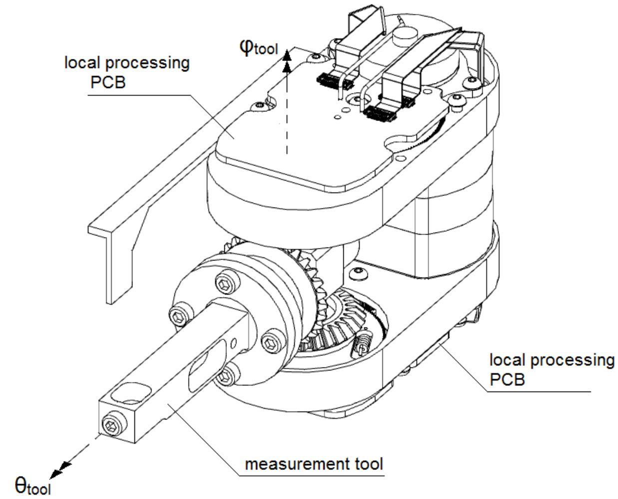


Fig. 4. A single 2DOF module with indicated $\phi_{tool}$-axis (pitch) and $\theta_{tool}$-axis (roll). A measurement tool is attached to the outgoing axis of the module. Mirrors are placed on the tool to reflect the laser beam of an external measurement device during precision tests.

With $\boldsymbol{K}$, a diagonal controller, the open-loop system $\boldsymbol{KL}$ has in- and outputs roll and pitch. The decoupled system is identified using system identification techniques to retrieve the frequency response functions of the roll and pitch motions. Using loop shaping, the feedback loops are sequentially closed and the bandwidth is set to $\pm 10$ Hz using PID-controllers.

The friction present in the drive train of the modules is compensated by a feed-forward. Coulomb and viscous friction have been identified by requiring each driven gear to track a constant velocity profile and by measuring the corresponding motor torque. Next, the break-away torque is measured for each position of the driven gears. Results in Fig. 6 show a position-dependent friction map for movements in positive and negative direction. The corresponding motor torque data has been used to create a lookup table. Recurrence of the gear teeth is clearly visible in the friction profile.

A block diagram of the complete control architecture for a single 2DOF module is shown in Fig. 5. The feedback controller $\boldsymbol{K}$ "sees" the decoupled plant $\boldsymbol{L}$ as given by (1), while the friction compensator acts on $\boldsymbol{G_{mod}}$ directly.

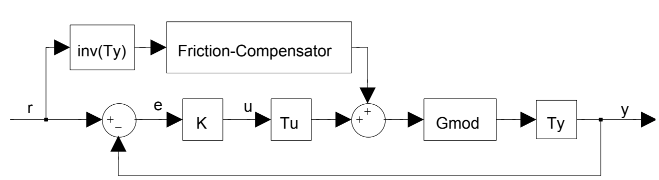


Fig. 5. The block diagram shows the control architecture of a single 2DOF module. The feedback controller $\boldsymbol{K}$ controls the decoupled plant. The friction compensator accounts for the friction inside the drive trains.

## III. Results

A test setup has been designed, comprising a 2DOF module, mounted on a measurement frame. An autocollimator and laser vibrometer are used to externally measure the position of a measurement tool containing reflective surfaces (Fig. 4).

### A. Tracking Performance

The tracking performance of a single 2DOF module with and without friction compensation is shown in Fig. 7. The measurement tool is set to track a sinusoidal reference signal around $\theta_{tool}$ with a frequency of 0.1 Hz and amplitude of 0.14 radians and zero reference around $\phi_{tool}$. A position feedback controller (PID) with a bandwidth of 20 Hz is used. Without feed-forward, the maximum tracking error is equal to 14 mrad, i.e. 10% of the reference signal amplitude. Position-dependent friction feed forward reduces the maximum tracking error by a factor of 8, i.e. a maximum error equal to 1.7 mrad (1.2% of reference signal amplitude).

### B. Bidirectional Precision

In this experiment the $\phi_{tool}$-movement of the bevel gear is set to zero, while the $\theta_{tool}$-direction is slowly driven to a reference value several times, from positive and negative offsets. The resulting steady-state angular error corresponding to each step is translated to a positional error at the tip of the end effector link (located at a distance of 160 mm from the $\phi_{tool}$-axis, and 160 mm from the $\theta_{tool}$-axis). Fig. 8 presents the results when the positional error is measured by the internal encoders (Nemo3 [20]) and by external measurements done by a combination of a laser vibrometer and autocollimator. The modules' internal encoder data indicate a bidirectional precision of 9 µm, whereas the external measurement devices indicate a variation of 70 µm. The gap between the data points from the absolute measurement devices, indicates the presence of play. The difference in variation of measurement points along the actuated degree of freedom, provided by the internal Nemo3 encoder and the absolute measurement devices, is caused mainly by friction in the drive train. A part of this friction has been compensated for by the position-dependent feed-forward.

Around the non-actuated $\phi_{tool}$-axis, bidirectional precision is equal to 21 µm according to the internal Nemo3 encoders and 22 µm for the absolute measurement devices. Variation along the non-actuated axis of rotation can be considered as an artifact of the actuated degree of freedom.

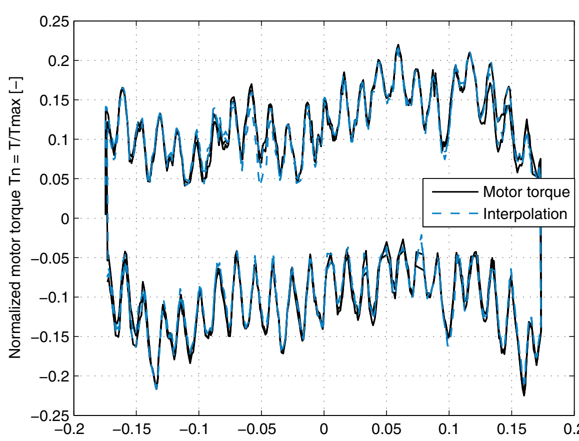


Fig. 6. Position-dependent normalized motor torque, representing the Coulomb friction in the drive train. The solid line is the average of four measurements and the dashed line is a linear interpolation.

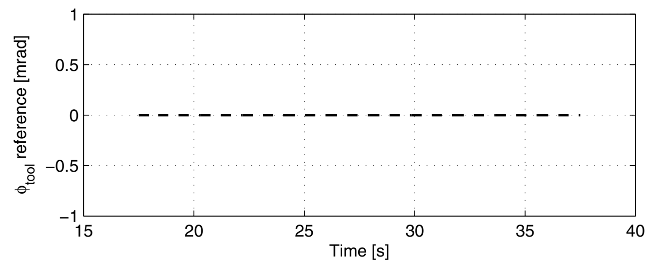


(a) Reference signal for $\phi_{tool}$.

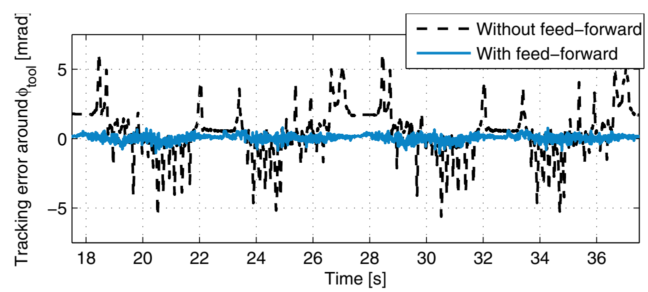


(b) Error signal for $\phi_{tool}$.

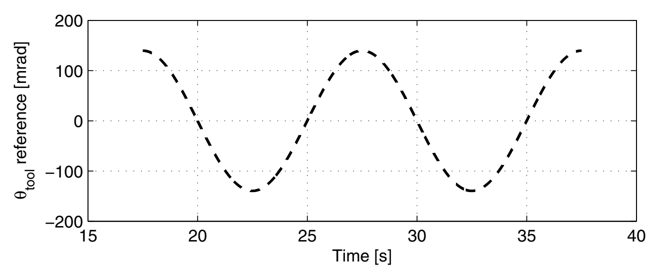


(c) Reference signal for $\theta_{tool}$.

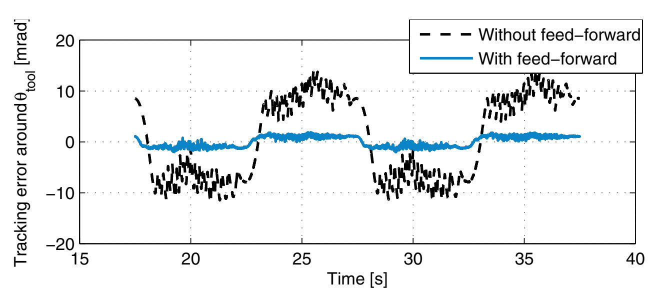


(d) Error signal for $\theta_{tool}$.

Fig. 7. The driven bevel gear is to follow a sinus reference signal (0.1 Hz and 0.14 radians amplitude) in $\theta_{tool}$-direction (Fig. 7c) and zero reference in $\phi_{tool}$-direction (Fig. 7a). Without feed-forward, the magnitude of the tracking error is shown by the dashed line (Fig. 7b,7d). The tracking error decreases a factor 10 with enabled feed-forward (solid line).

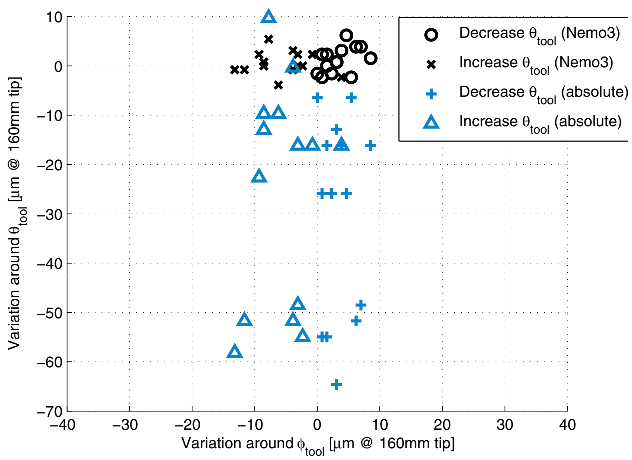


Fig. 8. The measurement tool is actuated around the $\theta_{tool}$ axis, to a certain encoder setpoint and back to the reference position until the system is at rest. Final position of the measurement tool is measured by the Nemo3 encoder (○/×) and by a combination of laser vibrometer and autocollimator (+/△). The error with respect to the reference position is logged.

## IV. Conclusions and Future Work

In this paper a novel 7DOF master-slave system is introduced. The system allows surgeons to use conventional microsurgical approaches and techniques, whereas the OR setup remains unchanged. Because of the small size and weight, backdrivable gear trains, and balanced manipulator mechanism, an inherently safe system is realized. Up to four slave manipulators can be mounted to a central ring-shaped suspension, allowing multiple surgeons to work cooperatively in the same operation site. The mechanical design of the manipulators is highly symmetrical, which leads to low production costs. A proof-of-concept of the system has been used to perform a number of tests, whereas preliminary results indicate a bidirectional precision at the slave end effector equal to 70 μm. The system is functionally operating, but further optimization needs to be done. As a next step, tests should be performed by surgeons in a non-clinical setting, to indicate if the system is suitable for use during microsurgical procedures. After that, a phase of clinical test procedures should be planned. The current gear transmission imposes a limit of 30−40 μm on the precision that can be achieved at the end effector, mainly because of the occurring friction and play. Mechanical optimization (e.g other gear configurations or materials) or alternative drive train solutions are expected to lead to a significant increase in performance. Using feedback from surgeons, the current proof-of-concept model will be developed further, to create a system that is highly dedicated to reconstructive microsurgery applications.

## References


[1] J.-F. Daneault, B. Carignan, and C. Duval, "Finger tremor can be voluntarily reduced during a tracking task," *Brain research*, vol. 1370, pp. 164–174, 2011.

[2] T. S. Wells, S. Yang, R. A. MacLachlan, J. T. Handa, P. Gehlbach, and C. Riviere, "Comparison of baseline tremor under various microsurgical conditions," in *Systems, Man, and Cybernetics (SMC), 2013 IEEE International Conference on*. IEEE, 2013, pp. 1482–1487.

[3] K. Veluvolu and W. Ang, "Estimation and filtering of physiological tremor for real-time compensation in surgical robotics applications," *The International Journal of Medical Robotics and Computer Assisted Surgery*, vol. 6, no. 3, pp. 334–342, 2010.

[4] J. P. Hong, "The use of supermicrosurgery in lower extremity reconstruction: the next step in evolution," *Plastic and reconstructive surgery*, vol. 123, no. 1, pp. 230–235, 2009.

[5] I. Koshima, "Atypical arteriole anastomoses for fingertip replantations under digital block," *Journal of Plastic, Reconstructive & Aesthetic Surgery*, vol. 61, no. 1, pp. 84–87, 2008.

[6] S. Charles, H. Das, T. Ohm, C. Boswell, G. Rodriguez, R. Steele, and D. Istrate, "Dexterity-enhanced telerobotic microsurgery," in *Advanced Robotics, 1997. ICAR'97. Proceedings., 8th International Conference on*. IEEE, 1997, pp. 5–10.

[7] D. F. Louw, T. Fielding, P. B. McBeth, D. Gregoris, P. Newhook, and G. R. Sutherland, "Surgical robotics: a review and neurosurgical prototype development," *Neurosurgery*, vol. 54, no. 3, pp. 525–537, 2004.

[8] R. A. MacLachlan, B. C. Becker, J. Cuevas Tabares, G. W. Podnar, L. A. Lobes, and C. N. Riviere, "Micron: an actively stabilized handheld tool for microsurgery," *Robotics, IEEE Transactions on*, vol. 28, no. 1, pp. 195–212, 2012.

[9] B. Mitchell, J. Koo, M. Iordachita, P. Kazanzides, A. Kapoor, J. Handa, G. Hager, and R. Taylor, "Development and application of a new steady-hand manipulator for retinal surgery," in *Robotics and Automation, 2007 IEEE International Conference on*. IEEE, 2007, pp. 623–629.

[10] C. Taleb, E. Nectoux, and P. Liverneaux, "Telemicrosurgery: a feasibility study in a rat model," *Chirurgie de la main*, vol. 27, no. 2, pp. 104–108, 2008.

[11] J. Schiff, P. S. Li, and M. Goldstein, "Robotic microsurgical vasovasostomy and vasoepididymostomy: a prospective randomized study in a rat model," *The Journal of urology*, vol. 171, no. 4, pp. 1720–1725, 2004.

[12] E. Nectoux, C. Taleb, and P. Liverneaux, "Nerve repair in telemicrosurgery: an experimental study," *Journal of reconstructive microsurgery*, vol. 25, no. 04, pp. 261–265, 2009.

[13] W. Kuang, P. R. Shin, S. Matin, and A. J. THOMAS JR, "Initial evaluation of robotic technology for microsurgical vasovasostomy," *The Journal of urology*, vol. 171, no. 1, pp. 300–303, 2004.

[14] R. D. Katz, J. A. Taylor, G. D. Rosson, P. R. Brown, and N. K. Singh, "Robotics in plastic and reconstructive surgery: use of a telemanipulator slave robot to perform microvascular anastomoses," *Journal of reconstructive microsurgery*, vol. 22, no. 01, pp. 053–058, 2006.

[15] J. C. Selber, G. Robb, J. M. Serletti, G. Weinstein, R. Weber, and F. C. Holsinger, "Transoral robotic free flap reconstruction of oropharyngeal defects: a preclinical investigation," *Plastic and reconstructive surgery*, vol. 125, no. 3, pp. 896–900, 2010.

[16] N. Maire, K. Naito, T. Lequint, S. Facca, S. Berner, and P. Liverneaux, "Robot-assisted free toe pulp transfer: Feasibility study," *Journal of reconstructive microsurgery*, vol. 28, no. 07, pp. 481–484, 2012.

[17] A. Morita, S. Sora, M. Mitsuishi, S. Warisawa, K. Suruman, D. Asai, J. Arata, S. Baba, H. Takahashi, R. Mochizuki *et al.*, "Microsurgical robotic system for the deep surgical field: development of a prototype and feasibility studies in animal and cadaveric models," *Journal of neurosurgery*, vol. 103, no. 2, pp. 320–327, 2005.

[18] M. Mitsuishi, A. Morita, N. Sugita, S. Sora, R. Mochizuki, K. Tanimoto, Y. M. Baek, H. Takahashi, and K. Harada, "Master–slave robotic platform and its feasibility study for micro-neurosurgery," *The International Journal of Medical Robotics and Computer Assisted Surgery*, 2012.

[19] R. Cau, "Design and realization of a master-slave system or reconstructive microsurgery," Ph.D. dissertation, Eindhoven University of Technology, 2013.

[20] N. J. GmbH. (2013) Numerik jena. [Online]. Available: http://www.numerikjena.com/